Maximizing Yield with Improved Single-Axis Backtracking on Cross-Axis Slopes

Preprint

Kevin Anderson

National Renewable Energy Laboratory

Presented at the 47th IEEE Photovoltaic Specialists Conference (PVSC 47)
June 15 - August 21, 2020

NREL is a national laboratory of the U.S. Department of Energy
Office of Energy Efficiency & Renewable Energy
Operated by the Alliance for Sustainable Energy, LLC

This report is available at no cost from the National Renewable Energy Laboratory (NREL) at www.nrel.gov/publications.

Contract No. DE-AC36-08GO28308

Conference Paper
NREL/CP-5K00-76023
June 2020

Maximizing Yield with Improved Single-Axis Backtracking on Cross-Axis Slopes

Preprint

Kevin Anderson

National Renewable Energy Laboratory

Suggested Citation
Anderson, Kevin. 2020. *Maximizing Yield with Improved Single-Axis Backtracking on Cross-Axis Slopes: Preprint*. Golden, CO: National Renewable Energy Laboratory. NREL/CP-5K00-76023. https://www.nrel.gov/docs/fy20osti/76023.pdf.

Conference Paper
NREL/CP-5K00-76023
June 2020

National Renewable Energy Laboratory
15013 Denver West Parkway
Golden, CO 80401
303-275-3000 • www.nrel.gov

NOTICE

This work was authored by Alliance for Sustainable Energy, LLC, the manager and operator of the National Renewable Energy Laboratory for the U.S. Department of Energy (DOE) under Contract No. DE-AC36-08GO28308. Funding provided by the U.S. Department of Energy's Office of Energy Efficiency and Renewable Energy (EERE) under Solar Energy Technologies Office (SETO) Agreement Number 34348. The views expressed in the article do not necessarily represent the views of the DOE or the U.S. Government. The U.S. Government retains and the publisher, by accepting the article for publication, acknowledges that the U.S. Government retains a nonexclusive, paid-up, irrevocable, worldwide license to publish or reproduce the published form of this work, or allow others to do so, for U.S. Government purposes.

Cover Photos by Dennis Schroeder: (clockwise, left to right) NREL 51934, NREL 45897, NREL 42160, NREL 45891, NREL 48097, NREL 46526.

Maximizing Yield with Improved Single-Axis Backtracking on Cross-Axis Slopes

Kevin Anderson
National Renewable Energy Laboratory
Golden, USA
kevin.anderson@nrel.gov

***Abstract*—Many tracking PV systems avoid row-to-row shading by backtracking in morning and afternoon. Because the common single-axis backtracking implementation assumes the array is in a horizontal plane, it does not fully prevent row-to-row shading in arrays installed on cross-axis slopes, e.g. an east-west slope for a tracker with north-south axis alignment. This paper presents the simulated effect of reduced self-shading on annual production with two modified backtracking strategies. Depending on the array geometry and the steepness of the cross-axis grade, using a modified backtracking strategy improved annual yield by 3-10%.**

***Index Terms*—single-axis tracking, backtracking, photovoltaic, shading, slope, grade, yield**

I. Introduction

Single-axis trackers are commonly used in large-scale photovoltaic installations because of their improved insolation capture compared with fixed-tilt arrays. The basic tracking algorithm (called "true-tracking") minimizes the incidence angle between the panel normal and incoming beam irradiance from the sun. This approach lays modules flat at solar noon and tilts modules at steep angles in early morning and late afternoon to face towards the sun when it is at low elevation. At steep tilt and low sun elevation, inter-row shading creates cell to cell electrical mismatch in modules with a conventional cell layout, resulting in severe nonlinear power loss. To avoid this power loss, the tracking algorithm is modified to lay modules flatter as the sun approaches the horizon to prevent row-to-row shading. This modified behavior in morning and evening is called "backtracking" because of the reversed tracking direction during those times [1]. The backtracking behavior implemented in most trackers is dependent only on the array ground coverage ratio (GCR) and implicitly assumes the array is installed on flat terrain. As such, the common backtracking implementation fails to prevent self-shading in arrays built on cross-slopes where adjacent rows are vertically offset from each other. For example, a tracker array with north-south axis built on a west-facing slope would have to backtrack more than usual in the morning to avoid self-shading from the height difference between rows.

Previous work has compared backtracking geometries in flat arrays and sloped arrays [2]–[4] but did not investigate the effect on energy production. In this paper, the ideal cross-slope backtracking method is compared against the standard "flat backtracking" method and an "adjusted-GCR" backtracking method using a photovoltaic performance model to determine the effect on annual energy production. Note that these three strategies focus on presenting the optimal angle to direct irradiance while avoiding self-shading in an attempt to maximize PV production. However, capture of direct irradiance is an imperfect proxy for PV production; in diffuse-dominated conditions, production might be maximized by laying trackers flat to improve collection of downwelling diffuse irradiance. Laying trackers flat in overcast conditions has been estimated to improve production by up to 2.5% in overcast climates [5]. However, the strategies considered here have the advantage that they are implemented purely in software in the tracker controllers; no additional hardware is needed to measure the diffuse fraction of available irradiance or other optimization criteria.

Section II describes the three strategies considered here. Section III describes the PV power and partial shading loss models used in this analysis. Finally, Section IV presents an overall production comparison of the three strategies.

II. Backtracking Strategies

This section describes the three backtracking strategies considered in this analysis. The first is the "standard" backtracking routine widely used in deployed tracker systems today as described in [1]. The second uses the same equations as the first but with a different GCR from the array's true GCR. The third is the slope-aware backtracking routine described in [4].

The qualitative behavior of each method is described in terms of irradiance capture and self-shading on the "upslope" and "downslope" parts of the day, which refer to the halves of the day (morning or afternoon) when the sun is on the uphill and downhill side of the array, respectively.

In each case, the backtracking angle θ_B is calculated as the sum of the true-tracking angle θ_T and a backtracking correction angle θ_c:

$$\theta_B = \theta_T + \theta_c \tag{1}$$

Each of the three methods yields a value for θ_c given the required array geometry and true-tracking angle θ_T (which

is defined identically across each of the three strategies because it does not consider array geometry).

A. Standard Backtracking

As presented in [1], the standard backtracking correction angle is defined simply by

$$\cos\theta_c = -\frac{\cos\theta_T}{\mathrm{GCR}} \tag{2}$$

At sunrise and sunset when $|\theta_T| \to 90°$, $|\theta_c| \to 90°$ as well, resulting in $\theta_B \to 0$. In the case of a cross-axis slope, this backtracking method is conservative on the downslope side of the day because it remains flat even though the vertical offset between rows would permit a steeper tilt without self-shading. It also fails to prevent shading on the upslope part of the day because the vertical offset places the lower edge of each module below where the standard backtracking equation expects it to be.

B. Adjusted-GCR Backtracking

As mentioned earlier, the adjusted-GCR method uses the standard backtracking correction equation but with a modified GCR value. The idea is that because the standard backtracking approach fails on a cross-slope and the backtracking routine only takes one parameter (GCR), changing the GCR value programmed into the tracker controller might avoid some of the shading. This method has the advantage that it doesn't require a firmware update to the tracker controllers to implement, only a change to the GCR value configured in the controller interface. However, it's not necessarily clear how to choose the value of the GCR adjustment (the method is a trade-off between reduced shading loss and reduced irradiance capture), and no matter the chosen adjustment, this method can only ever be an imperfect solution because the limiting behavior is still to lay flat at sunrise and sunset. Despite its limitations, it is a workaround for systems that are unable to use the ideal method because of limitations in the tracker controller.

A brute-force sweep can be used to find the optimal adjusted GCR for a given system specification and location. The results of such a sweep are presented in Section IV-A.

C. Ideal (Slope-Aware) Backtracking

The ideal backtracking method can be derived intuitively by applying a rotation of the cross-axis slope angle β_c around the tracker axis to Equation 2 to accommodate the cross-axis slope. Here is the equation derived in [4], which includes some extra modifications to correctly handle tilted tracker axes:

$$\theta_c = -\mathrm{sign}\,\theta_T \arccos\left[\frac{|\cos(\theta_T + \beta_c)|}{\mathrm{GCR}\cos\beta_c}\right] \tag{3}$$

Note that rotating the system plane not only shifts θ_T by the rotation angle but also changes the horizontal spacing between rows and therefore the GCR as well, requiring the $\cos\beta_c$ term in the denominator. Here, as in [4], GCR is defined according to the axis spacing in the horizontal plane.

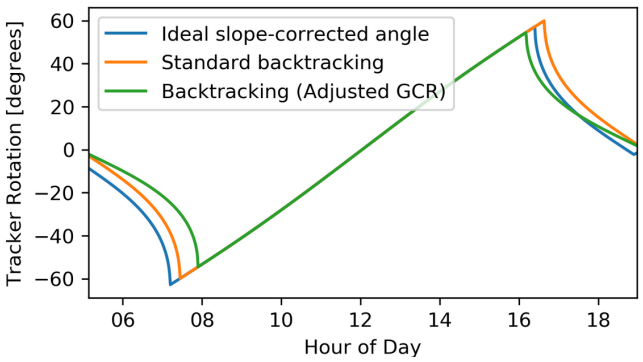

Fig. 1. Three tracking algorithms for a hypothetical array on an East-facing slope. Orange line: standard backtracking (GCR = 0.5); green line: adjusted-GCR backtracking (GCR = 0.58); blue line: ideal backtracking (GCR = 0.5, $\beta_c = 3°$)

Figure 1 compares a daily rotation curve using standard flat-terrain backtracking, adjusted-GCR backtracking, and ideal backtracking for a system on an east-facing slope. By comparing the first two curves to the ideal curve it is possible to see when shading occurs for each strategy. In the afternoon after the system starts to backtrack, the standard curve is always at a steeper tilt than the ideal curve, indicating continuous partial shading. The adjusted-GCR curve avoids much of the shading in the afternoon, but does eventually cross over the ideal curve and begin self-shading near the end of the day. However, this comes at the price of significantly worse positioning in the morning. Neither of the slope-naive methods is able to accommodate the broken morning/evening symmetry between shading and backtracking angle. However, the ideal method tilts more steeply towards the sun in the morning (including as soon as the sun comes above the horizon) while still avoiding row-to-row shading and backtracks as little as necessary in the afternoon. Note that for this example, the adjusted GCR was chosen somewhat arbitrarily by visually balancing shading avoidance with reduced irradiance capture.

III. Modeling PV Power Under Partial Shade

Although shading avoidance may have other benefits for PV arrays (for instance, preventing cells from entering reverse bias and experiencing accelerated degradation), this analysis studies the effect on annual energy production. Using the same weather data for each simulation, the annual energy production using standard backtracking, adjusted-GCR backtracking, and ideal backtracking are simulated and compared.

The modeling approach in each case is to model the expected power of an unshaded system and then apply a loss predicted from a partial shading model. The power generation for each tracking pattern is simulated using

the open source python package pvlib-python [6], [7]. The weather file used in this simulation is the year-long 2012 dataset recorded at the Goodwin Creek, Mississippi SURFRAD station [8]. SURFRAD ground station instrumentation is regularly maintained and reports high-quality continuous 1-minute meteorological measurements. In this case, we use the three irradiance measurements and the ambient temperature readings.

A. Partial Shading Loss

The general task of PV modeling under partial shade is fairly complex. In this context we can make several simplifying assumptions without significantly restricting the applicability of the results. First, we assume a standard 72-cell module with three "down-and-back" cell strings. We assume that row-to-row shading affects each cell string equally, so no consideration of bypass diodes is necessary. We also assume that row-to-row shading affects only direct irradiance, meaning all cells are exposed to the same diffuse irradiance. Finally, we assume that cell temperature is uniform across the module and modeled without consideration of the shading.

A high-accuracy method of modeling partial shading is to model IV curves for each cell separately according to the cell's shading conditions and combine the cell curves into a module-level curve. However, this process is very computationally intensive. Here we use a simpler model that is somewhat less accurate, but dramatically faster to compute. By making the approximation that a cell string's production is limited by its most shaded cell, we define a piecewise shading model:

$$P_{norm} = \begin{cases} 1 - (1 - f_d) f_s N & f_s < 1/N \\ f_d & f_s \geq 1/N \end{cases} \quad (4)$$

Here P_{norm} is the output power of the module as a fraction of the power it would produce without shade, f_d is the diffuse fraction of in-plane irradiance, f_s is the shaded fraction of the module, and N is the number of cells per column in the module. Assuming a standard 72-cell module, $N = 12$. Following the assumptions that each string is limited by its most shaded cell and each string performs equally, we model the most shaded cell and assume the rest of the module performs equally. The model is defined piecewise to handle the separate cases of when the bottom row of cells is only partially shaded ($f_s < 1/N$) and when the bottom row is fully shaded ($f_s \geq 1/N$). When the bottom row is only partially shaded, the power is decreased by the shaded fraction of the cell $f_s N$ according to the direct irradiance fraction $1 - f_d$. When it is fully shaded, the power is just equal to the diffuse fraction.

To validate this model, we benchmark it against a cell-level IV model as described earlier. We use the De Soto single-diode model presented in [9] for generating the five single-diode equation parameters at operating conditions.

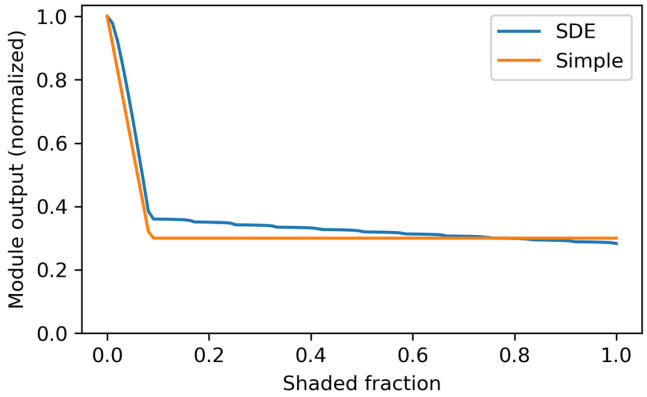

Fig. 2. Predicted power output of a partially shaded module using the simple shading model and the full single-diode equation (SDE). In both cases, the diffuse fraction is set to 0.3.

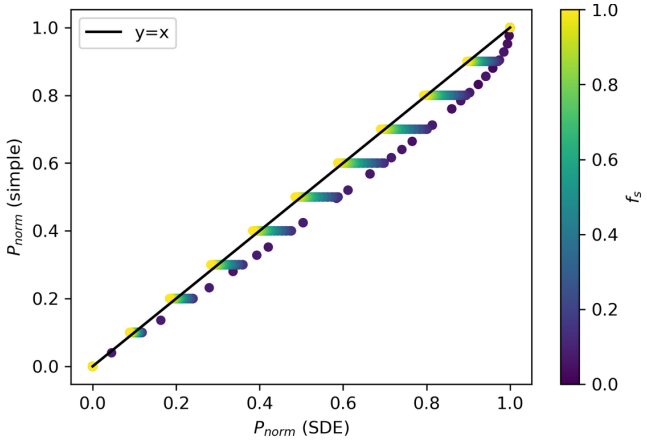

Fig. 3. Predicted power output of a partially shaded module using the simple shading model and the full single-diode equation (SDE). Points in the upper right have higher diffuse fraction (f_d) than points in the lower left. Shaded fraction (f_s) is shown by color.

We then use Bishop's method [10] to calculate the actual IV curves. Both of these steps are completed using the implementations in pvlib-python.

Figure 2 compares the output of a full single-diode model against the simple model as a function of shaded fraction. The simple model successfully captures the general behavior of the full single-diode model (initial steep drop in output power until one cell is fully shaded, then leveling out), although there is some error, especially where f_s is somewhat larger than $1/N$. Figure 3 shows a more complete comparison that sweeps across both f_s and f_d. Although the simple model does tend to overpredict shading loss (therefore underpredicting output power), the agreement is fairly good overall. We choose to use the simple shading model for the following analysis because the simple model is so much more computationally efficient than the cell-level IV curve modeling procedure and shows acceptably small error.

B. PV Power Modeling

For each timestamp in the irradiance dataset, the modeling process is as follows:

1) Calculate the standard, adjusted-GCR, and ideal backtracking angles.
2) Transpose the measured irradiance components into plane-of-array (POA) direct and diffuse components (using the isotropic diffuse sky model) for the three backtracking positions using pvlib-python. Irradiance losses from soiling and reflection are ignored.
3) Model cell temperature with the Sandia Array Performance Model [11] using thermal coefficients for the glass/cell/polymer, open rack configuration ($a = -3.56$, $b = -0.075$, $\Delta T = 3$).
4) Calculate the unshaded PV power using the PVWatts DC model [12], assuming a temperature coefficient of $\gamma_{pdc} = -0.43\%/C$.
5) Calculate the module shaded fractions [4].
6) Using the simple shading loss model described in Section III-A, calculate the shaded power.

Figure 4 compares the simulated PV power for each of the three backtracking strategies for an East-facing slope on a clear-sky day. In comparison to standard backtracking, adjusted-GCR backtracking avoids the majority of the afternoon shading loss (Region III), although it still experiences some shading loss (Region IV). Additionally, the adjusted-GCR method slightly reduces morning production (Region I). In contrast, ideal backtracking avoids all afternoon shading and improves morning irradiance capture, though the avoided shading has much greater effect than the improved irradiance capture.

IV. Results

The above modeling approaches were used for two analyses. The first is to find the optimal GCR to use with the adjusted-GCR method as a function of cross-axis grade and true array GCR. The second compares annual production for the three backtracking strategies across a range of GCR and cross-axis grades (using the optimal adjusted GCR in the adjusted-GCR method).

A. Adjusted-GCR optimization

To find the optimal adjusted GCR for the adjusted-GCR method, a brute force sweep across adjusted GCRs was performed. Figure 5 shows the results of this sweep applied for two cross-axis grades (0.05 and 0.15) for an array with a true GCR of 0.4. Interestingly, the annual production curve has local maxima on both sides of the true GCR. The choice to increase or decrease the adjusted GCR could be described as the tradeoff between (1) avoiding the majority of upslope shading without totally sacrificing downslope irradiance capture and (2) writing off the upslope part of the day as a total loss and optimizing for production on the downslope side. Another interesting result is the the global maximum is at an increased GCR for the mild slope but a decreased GCR for the steep slope.

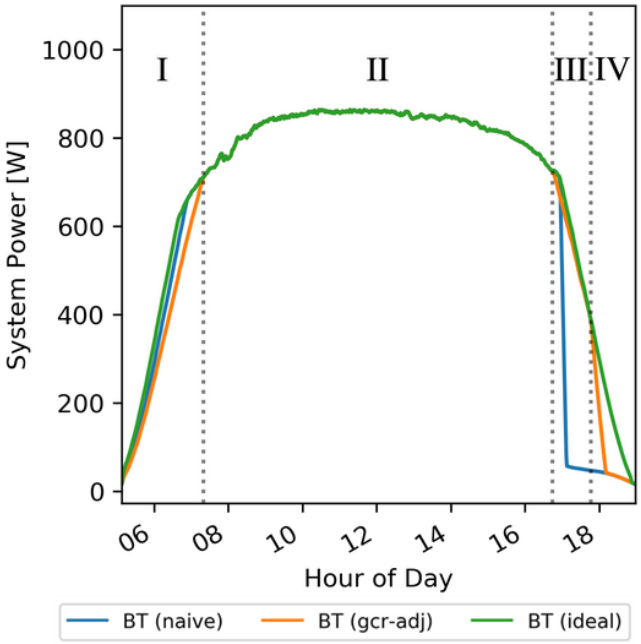

Fig. 4. Simulated PV power for standard ("naive") backtracking (blue), adjusted-GCR backtracking (orange), and ideal backtracking (green) for a clear-sky day (GCR = 0.4, grade = 0.05). In order, the numbered regions show (I) reduced irradiance capture by the non-ideal strategies; (II) identical production during the true-tracking part of the day; (III) avoided shading using the adjusted-GCR strategy; (IV) failed shading avoidance with the adjusted-GCR strategy.

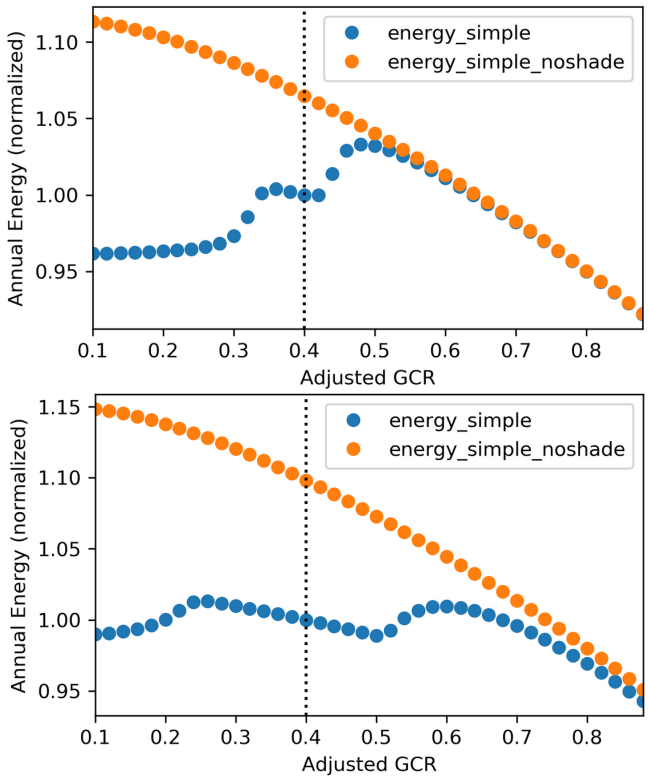

Fig. 5. Annual production using the adjusted-GCR method as a function of adjusted GCR. The unshaded power is shown for comparison. The y-axis shows annual production normalized by the production using the true GCR. Top: grade=0.05. Bottom: grade=0.15.

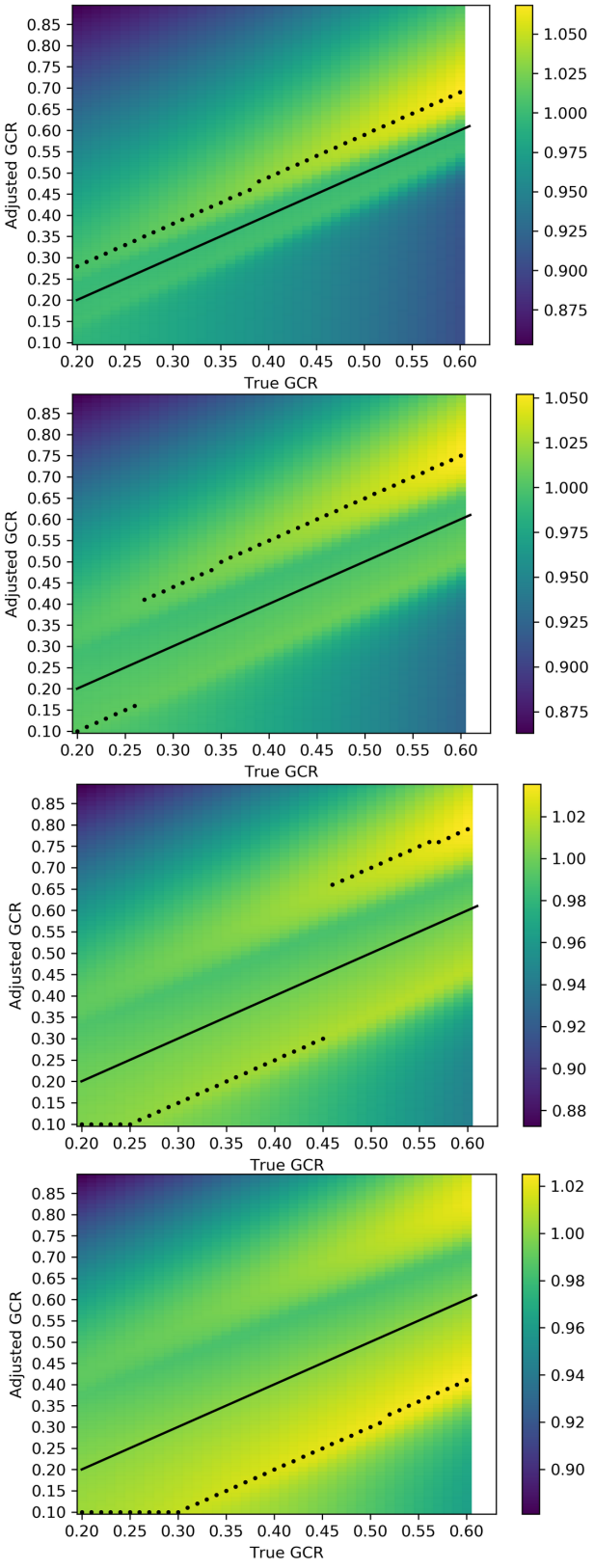

Fig. 6. Annual production heatmaps as a function of adjusted GCR and cross-axis grade. X-axis shows true array GCR, Y-axis shows adjusted GCR, and color shows annual production, normalized to the annual production for that true GCR. The optimal adjusted GCR for each true GCR is plotted as black dots. The solid line shows where adjusted GCR equals true GCR. From top to bottom: grade equals 0.05, 0.10, 0.15, 0.20.

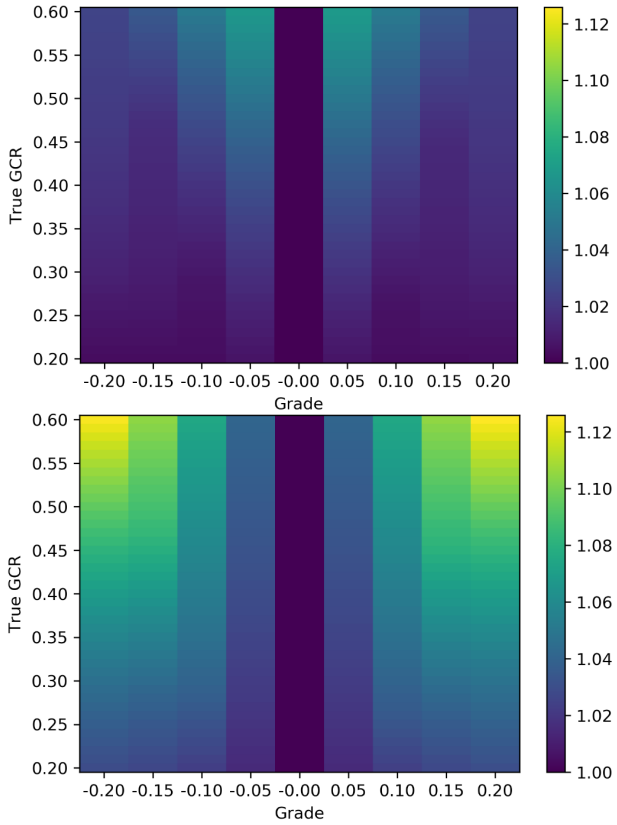

Fig. 7. Annual production gain heatmaps as a function of cross-axis grade and true GCR. Color shows the ratio of annual production between the two compared strategies for each (GCR, grade) pair. Top: production ratio between adjusted-GCR backtracking and standard backtracking. Bottom: production ratio between ideal backtracking and adjusted-GCR backtracking.

To further investigate this result, a similar sweep across adjusted GCRs was performed across the GCR range from 0.2 to 0.6 and from cross-axis grades from 0.0 to 0.2. The optimization results for each of these sweeps are shown in Figure 6. As grade increases, the optimal adjusted GCR is more likely to be less than the true GCR. Additionally, the optimal GCR appears to be offset a constant magnitude from the true GCR with the magnitude determined by the cross-axis grade.

B. Annual Production by Strategy

Using the optimal adjusted GCRs calculated above, the annual production of the three strategies are compared across GCRs and grades in Figure 7. The adjusted-GCR method performs well compared to the standard backtracking method, showing significant gains for mild cross-axis grades. However, the gain at steeper grades is much smaller. The ideal method shows a significant improvement over the adjusted-GCR method even in cases where the adjusted-GCR method performs well and especially where it performs poorly. For a "realistic" case (grade=0.05, GCR=0.4), the adjusted-GCR method shows a 4% improvement in annual production, with an

additional 3-4% on top (7-8% total) with ideal bactracking. For steeper slopes, the gain increases significantly.

Note that calling this production improvement a "gain" can be misleading because these gains are just partially recouping a loss. Implementing these strategies in a system with a typical no-shading energy model that is otherwise accurate will reduce the system's underperformance relative to the model, not cause it to overperform the model. Additionally, even with perfect shading avoidance, a tracking system on a cross-slope will likely underperform an otherwise identical system on flat terrain because of reduced insolation capture.

V. Conclusions

Modifying the backtracking behavior of tracker arrays on cross-axis slopes can prevent significant production losses associated with row-to-row shading. For the simplified case of constant cross-axis slope, the optimal backtracking GCR was found across a range of true array GCRs and cross-axis grades. Although the optimization was performed assuming constant slope over the array, the results are likely close to optimal for arrays on rolling terrain as well, though a more specific analysis may be worthwhile for systems with nonuniform grade. Simulated PV production for a high-quality year-long test irradiance dataset showed an increase in annual production of roughly 3% by backtracking according to an optimized programmed GCR for a PV array with realistic geometry (GCR = 0.4, grade = $\pm$0.05). This production improvement was roughly doubled by using the ideal backtracking method that considers both cross-axis slope and GCR. At steeper slopes and increased GCRs, the simulated production improvement increased dramatically. Because these algorithms do not rely on external hardware and can be implemented purely in software, they are expected to be widely applicable to single-axis tracking systems.

VI. Acknowledgement

This work was authored by Alliance for Sustainable Energy, LLC, the manager and operator of the National Renewable Energy Laboratory for the U.S. Department of Energy (DOE) under Contract No. DE-AC36-08GO28308. Funding provided by the U.S. Department of Energy's Office of Energy Efficiency and Renewable Energy (EERE) under Solar Energy Technologies Office (SETO) Agreement Numbers 34348. The views expressed in the article do not necessarily represent the views of the DOE or the U.S. Government. The U.S. Government retains and the publisher, by accepting the article for publication, acknowledges that the U.S. Government retains a nonexclusive, paid-up, irrevocable, worldwide license to publish or reproduce the published form of this work, or allow others to do so, for U.S. Government purposes.

References

[1] E. Lorenzo, L. Narvarte, and J. Muñoz, "Tracking and backtracking," *Progress in Photovoltaics: Research and Applications*, vol. 19, no. 6, pp. 747–753, 2011. [Online]. Available: https://doi.org/10.1002/pip.1085

[2] B. Nascimento, D. Albuquerque, M. Lima, and P. Sousa, "Backtracking algorithm for single-axis solar trackers installed in a sloping field," *International Journal of Engineering Research and Applications*, vol. 5, p. 100, December 2015.

[3] D. Schneider, "Control algorithms for large-scale single-axis photovoltaic trackers." *Acta Polytechnica*, vol. 52, no. 5, 2012.

[4] K. Anderson and M. Mikofski, "Slope-aware back-tracking for single-axis trackers," National Renewable Energy Laboratory, Golden, CO, Tech. Rep. NREL/TP-5K00-76626, 2020, in press.

[5] J. Antonanzas, R. Urraca, F. M. de Pison, and F. Antonanzas, "Optimal solar tracking strategy to increase irradiance in the plane of array under cloudy conditions: A study across Europe," *Solar Energy*, vol. 163, pp. 122 – 130, 2018. [Online]. Available: https://doi.org/10.1016/j.solener.2018.01.080

[6] W. Holmgren *et al.*, "pvlib/pvlib-python v0.7.0," https://doi.org/10.5281/zenodo.3585619, December 2019, zenodo.

[7] W. Holmgren, C. Hansen, and M. Mikofski, "pvlib python: a python package for modeling solar energy systems," *Journal of Open Source Software*, vol. 3, no. 29, p. 884, 2018. [Online]. Available: https://doi.org/10.21105/joss.00884

[8] J. A. Augustine, J. J. DeLuisi, and C. N. Long, "SURFRAD - a national surface radiation budget network for atmospheric research," *Bulletin of the American Meteorological Society*, vol. 81, no. 10, pp. 2341–2358, 2000. [Online]. Available: https://doi.org/10.1175/1520-0477(2000)081<2341:SANSRB>2.3.CO;2

[9] W. D. Soto, S. Klein, and W. Beckman, "Improvement and validation of a model for photovoltaic array performance," *Solar Energy*, vol. 80, no. 1, pp. 78–88, Jan. 2006. [Online]. Available: https://doi.org/10.1016/j.solener.2005.06.010

[10] J. Bishop, "Computer simulation of the effects of electrical mismatches in photovoltaic cell interconnection circuits," *Solar Cells*, vol. 25, no. 1, pp. 73–89, Oct. 1988. [Online]. Available: https://doi.org/10.1016/0379-6787(88)90059-2

[11] D. L. King, W. E. Boyson, and J. A. Kratochvil, "Photovoltaic array performance model," Tech. Rep. SAND Report 3535, August 2004.

[12] A. P. Dobos, "PVWatts version 5 manual," National Renewable Energy Laboratory, Golden, CO, Tech. Rep. NREL/TP-6A20-62641, 9 2014.